International Environmental Modelling and Software Society (iEMSs)
2010 International Congress on Environmental Modelling and Software
Modelling for Environment's Sake, Fifth Biennial Meeting, Ottawa, Canada
David A. Swayne, Wanhong Yang, A. A. Voinov, A. Rizzoli, T. Filatova (Eds.)
http://www.iemss.org/iemss2010/index.php?n=Main.Proceedings

CFD and GFD Hybrid Approach for Simulation of Multi-Scale Coastal Ocean Flow

H. S. Tang[1,*], X. G. Wu[1,2]

[1]Dept. of Civil Eng., City College, City Univ. of New York, New York, NY 10031, USA
[2]Zhejiang Inst. of Hydraulics & Estuary, Hangzhou, Zhejiang 310020, China

Abstract: We propose to couple computational fluid dynamics (CFD) and geophysical fluid dynamics (GFD) methods to simulate multi-scale and multi-physics coastal flows. In particular, an unsteady, three-dimensional (3D), incompressible CFD model is coupled with the Unstructured Grid Finite Volume Coastal Ocean Model (FVCOM). The coupling is two-way and realized using domain decomposition method with Chimera overset grids, and the resulting hybrid system will be able to capture flow phenomena with spatial scales from centimeters to hundreds of kilometers. In order to demonstrate the feasibility and performance of the proposed hybrid system, simulations of effluents discharged into a river and a coastal region are presented, together with discussions on issues for its further development.

1. INTRODUCTION

Coastal ocean flow phenomena span a vast range of spatial and temporal scales. For instance, tropical waves may propagate with wavelengths of one thousand kilometers and periods of one month (Legeckis et al., 1983). Spatial sizes of Langmuir cells hanging below water surfaces range from one to one thousand meters (Weller et al., 1985; Thorpe, 2004). Flows around enormous numbers of swimming microorganism are restricted to scales of micrometers (Pedley, 1992). Here, the scales refer to observation scales such as characteristic length and time, or, process scales such as those in wavelet analysis (Kumar and Foufoula-Georgiou, 1997).

In the few past decades, a number of geophysical fluid dynamics (GFD) models have been developed for coastal ocean flows. For example, the Princeton Ocean Model (POM), the Unstructured Grid Finite Volume Coastal Ocean Model (FVCOM), and the Hybrid Coordinate Ocean Model (HYCOM) were developed to predict currents, salinity, sea level, temperature, and turbulence distributions in the coastal ocean (Blumberg and Mellor, 1987; Chen et al., 2003; Halliwell, 2004). In recent years, computational fluid dynamics (CFD) approaches, which solve the full Navier-Stokes equations and can accurately model small scales and detailed flow structures, are now applied to flows with large ranges of scales (Tang et al., 2008). It should be pointed out that, although both GFD and CFD are based on the Navier-Stokes equations, they are different approaches with aspect to numerical technique, turbulence closure, and parameterization for small scales.

It is now urgently needed to accurately simulate coastal ocean flows because of emerging issues in economic development, human welfare, and military operations. Nevertheless, there is a great challenge in view of the fact that the flows happen at vastly different space and time scales and the efforts using numerical simulation have been greatly successful but, until now, merely at one, and occasionally two, space and time scales. The challenge comes from model restrictions, numerical techniques, and computer capabilities (Griffles et al., 2000; Dolbow et al., 2004). For instance, a deep ocean model has difficulty in dealing with the vertical mesh at sudden bathymetry changes as well as the smaller scales of nearshore

[*] Correspondence: htang@ccny.cuny.edu

flows (Song and Hou, 2006; Heimusund and Berntsen, 2006). Limitations such as hydrostatic assumptions and/or two-dimensionality of GFD models are inherent restrictions that prohibit accurate simulations of many important phenomena such as vertical motions of Langmuir cells. Although in principle CFD approaches have no such limitations and can capture flow phenomena at various scales, they are prohibitively expensive and not applicable in simulating actual coastal ocean flows.

Multi-physical/multi-scale modeling provides accurate simulation of coastal ocean flows, and it is becoming a trend in prediction of coastal ocean flows in recent years (Dolbow et al., 2004; Fringer et al., 2006; Tang et al., 2009). It is commonly recognized that a single, comprehensive model capable of dealing with multi-physical/multi-scale problems is unlikely in the near future. Nevertheless, given the fact that computer modeling has reached the point where the simulation of flows over relatively narrow ranges of scales has become mature, the hybrid method (HM), together with domain decomposition method (DDM), is one of the most promising currently available techniques to bridge the scales and overcome difficulties in multi-scale/multi-physics modeling (Benek et al., 1983; Harten, 1993; Dolbow et al., 2004). By HM and DDM, a flow domain will be divided into many subdomains, and each of them is assigned to an individual model, which is coupled with others used for its neighbor subdomains. A crucial as well as challenging issue in HM is coupling of solutions obtained using the individual models at the interfaces between them.

This paper describes a multi-scale/multi-physics approach for coastal ocean flow prediction, which couples CFD and GFD models using HM and DDM with Chimera overset grids, and it presents numerical examples to demonstrate its feasibility. Particularly, a three-dimensional (3D), unsteady, incompressible CFD model is coupled with the FVCOM model (e.g., Chen et al., 2003; Tang et al., 2008). The proposed approach is illustrated in simulations of effluent released from discharge ports with diameters of order centimeters into a river with kilometer in width, and the simulations results are compared with those obtained with pure CFD. In addition, modeling of such discharge with higher temperature into a coastal flow environment using the HM approach is presented, together with discussions on further development of the proposed hybrid approach.

2. GOVERNING EQUATIONS

The governing equations of the CFD models are the 3D continuity and Navier-Stokes equations that, in general curvilinear coordinates, are expressed as follows:

$$\Gamma \frac{\partial Q}{\partial t} + J \frac{\partial}{\partial \xi^k}(F^k - F_v^k) + H = 0, \tag{1}$$

where

$$\Gamma = diag(0,1,1,1), \qquad Q = (p,u,v,w)^T,$$

$$F^k = \frac{1}{J}(U^k, uU^k + p\xi_x^k, vU^k + p\xi_y^k, wU^k + p\xi_z^k)^T, \tag{2}$$

$$F_v^k = \frac{1}{J}\left(\frac{1}{\mathrm{Re}} + \nu_t\right)(0, g^{lk}\frac{\partial u}{\partial \xi^l}, g^{lk}\frac{\partial v}{\partial \xi^l}, g^{lk}\frac{\partial w}{\partial \xi^l})^T, \quad H = -\frac{T}{Fr^2}e.$$

The governing equation for heat transfer reads as

$$\frac{1}{J}\frac{\partial T}{\partial t} - \frac{\partial}{\partial \xi^k}\left\{\frac{1}{J}\left(\frac{1}{\mathrm{Pr}\,\mathrm{Re}} + \frac{\nu_t}{\mathrm{Pr}_t}\right)g^{lk}\frac{\partial T}{\partial \xi^l}\right\} = 0. \tag{3}$$

In the equations, t is the time, and $k,l = 1,2$, and 3, which correspond to the Cartesian coordinates x, y, and z, respectively. Here and hereafter, repeated indices imply summation. e is the unit in the gravity direction. p is the static pressure divided by the

density, *u*, *v*, and *w* are the Cartesian velocities in x, y, and z direction, respectively, and T is the temperature. ξ^k are the curvilinear coordinates, U^k ($=u_i\xi^i_{x_k}$, *i=1,2,3*) are the contravariant velocities in ξ^k directions, and u_i are respectively *u*, *v*, and *w* when *i=1, 2,* and *3*. Besides, $\xi^i_{x_k}$ is the metrics of the geometric transformation, *J* is the determinant of Jacobian of the geometric transformation $J=|\partial x_i/\partial\xi^j|$, and g^{ij} ($g^{ij}=\xi^i_{x_k}\xi^j_{x_k}$) is the contravariant metric tensor. *Re* is the Reynolds number, *Fr* is the Froude number, and *Pr* is the Prandtl number. ν_t is the turbulence eddy viscosity, and Pr_t is the turbulent Prandtl number. The standard mixing length model is used in this work (Tang et al., 2008).

In the FVCOM model, the governing equations are the continuity and momentum equations. The model consists of an external mode and an inner mode. The governing equations for the external mode are vertically averaged two-dimensional (2D) continuity and momentum equations:

$$\frac{\partial\eta}{\partial t}+\frac{\partial DU_l}{\partial x_l}=0, \tag{4}$$

$$\frac{\partial U_iD}{\partial t}+\frac{\partial U_iU_lD}{\partial x_l}=-gD\frac{\partial\eta}{\partial x_i}-\frac{gD}{\rho_0}\left(\int_{-1}^{0}\frac{\partial}{\partial x_i}\left(D\int_{\sigma}^{0}\rho d\sigma'\right)d\sigma+\frac{\partial D}{\partial x_i}\int_{-1}^{0}\sigma\rho d\sigma\right) \tag{5}$$
$$+(-1)^i fU_jD+\frac{\tau_{sx_i}-\tau_{bx_i}}{\rho_0}+D\tilde{F}_i+G_i,$$

$$G_i=\frac{\partial U_iU_lD}{\partial x_l}-D\tilde{F}_i-\left(\frac{\partial u_iu_lD}{\partial x_l}-D\overline{F}_i\right),\ D\tilde{F}_i\approx\frac{\partial}{\partial x_l}\left(\overline{A}_mH\left(\frac{\partial U_i}{\partial x_l}+\frac{\partial U_l}{\partial x_i}\right)\right),$$

$$D\overline{F}_i\approx\frac{\partial}{\partial x_l}\left(A_mH\left(\frac{\partial u_i}{\partial x_l}+\frac{\partial u_l}{\partial x_i}\right)\right), \tag{6}$$

and the governing equations of the internal mode are 3D continuity and momentum equations with x and y as horizontal coordinates and σ as vertical coordinate:

$$\frac{\partial\eta}{\partial t}+\frac{\partial Du_l}{\partial x_l}+\frac{\partial\omega}{\partial\sigma}=0, \tag{7}$$

$$\frac{\partial u_iD}{\partial t}+\frac{\partial u_iu_lD}{\partial x_l}+\frac{\partial u_i\omega}{\partial\sigma}=-gD\frac{\partial\eta}{\partial x_i}-\frac{gD}{\rho_0}\left(\frac{\partial}{\partial x_i}\left(D\int_{\sigma}^{0}\rho d\sigma'\right)+\sigma\rho\frac{\partial D}{\partial x_i}\right) \tag{8}$$
$$+(-1)^i fu_j+\frac{1}{D}\frac{\partial}{\partial\sigma}\left(K_m\frac{\partial u_i}{\partial\sigma}\right)+DF_i,$$

$$DF_i\approx\frac{\partial}{\partial x_l}\left(A_mH\left(\frac{\partial u_i}{\partial x_l}+\frac{\partial u_l}{\partial x_i}\right)\right). \tag{9}$$

In the FVCOM model, *i, j, l*=1,2 ($i\neq j$). η is the water surface elevation, and *D* and *H* are respectively water depth and mean of water depth. U_l are depth average velocities in x_l directions, ω is vertical velocity in σ coordinate. A_m and *K* are horizontal and vertical eddy viscosity, respectively, and they are determined using the Mellor and Yamada level-2.5 turbulent closure (Mellor and Yamada, 1982; Chen et al., 2003).

3. NUMERICAL METHODS AND COUPLING STRATEGY

In the CFD model, the governing equations are discretized using a second-order-accurate, implicit, finite-volume method on non-staggered grids, and they are solved using a dual time-stepping artificial compressibility method. The time derivative is approximated using the three-point backward differencing, the convective terms are discretized using the QUICK scheme, and the other terms are treated using central differencing. A third-order,

fourth-difference artificial dissipation method is employed to eliminate odd–even decoupling of the pressure field. The discretized system is integrated using an implicit, pressure-based pre-conditioner enhanced with the local-time-stepping and V-cycle multigrid method to accelerate convergence. A DDM approach using Chimera overset grids is implemented by which the flow domain is divided into subdomains arbitrarily overlapping with each other, each of them and is covered by a structured, body-fitted, curvilinear grid. Two-way coupling is enforced among subdomains, and the Schwartz alternative iteration is employed (Schwarz, 1869). In order to achieve seamless transition of solutions between subdomains, an effective mass conservation algorithm is proposed. For details about the technical aspects of the model, the reader is referred to Tang et al. (2003), Paik et al. (2005), and Tang (2006).

In the FVCOM, the flow domain is discretized using a triangle mesh on the horizontal plane and a layer mesh in the vertical direction. The governing equations are discretized using finite volume method. In both the 2D external mode and 3D internal mode, the convection terms are discretized using second-order accurate upwind schemes, and Runge-Kutta methods are used to march in time. In the solution procedure, first, the external mode is solved to obtain water surface elevation and horizontal average velocities, and then the internal mode is solved to predict velocity distributions. Second, in the internal mode, solving the momentum equations provides horizontal velocity distributions, which are then adjusted according to the horizontal average velocities obtained in external mode. Then, the vertical velocity component is obtained using the continuity equation in the internal mode. In order to maintain consistency between the internal and external modes, the vertical velocity is modified to ensure mass conservation at every time step. The external and internal modes may have different time steps. Details for the FVCOM model can be found in Chen et al. (2003) and Chen et al. (2006).

In this paper, the CFD model is employed to resolve local flow phenomena, and FVCOM is used to model background circulations. The solution domains of CFD and FVCOM and overlap in a certain region (Fig. 1). As seen in Eqs. (1), (2), (7), (8), and (9), CFD model solves for velocity u, v, and w, and the internal mode of the FVCOM model also provides solutions for them. Therefore, as a natural strategy, the CFD model is coupled to the internal mode of the FVCOM, and the two models exchange solutions for the velocity distributions at grid interfaces between them. The strategy is based on the assumption that the horizontal velocity distributions in the vertical direction do not directly affect water surface elevation and averaged values of horizontal velocities, and it is consistent with the assumption in FVCOM (Chen et al., 2003).

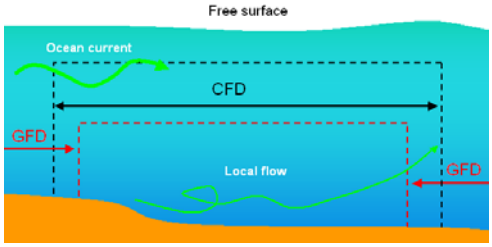

Figure 1. Schematic representation of CFD and GFD coupling

Chimera overset grids overlap arbitrarily with each other, and this method provides the best possible flexibility in connecting different models. In this research, Chimera overset grids are used between CFD and FVCOM models. At grid interfaces between the two models, the procedures and techniques described by Tang et al. (2003) and Tang (2006) are used in searching host cells in the CFD model grids (structured grids) for FVCOM interface grid nodes. Similar methods are employed in finding the host elements within the FVCOM model grid (triangle mesh in horizontal directions) for interface grid nodes of the CFD model. It is noted that the host cells do not change in horizontal plane during simulation of a flow. However, in view that FVCOM uses σ coordinate in vertical direction, the host cells may change as water surface elevation changes (unsteady flow). As a result, the relative positions of CFD and FVCOM grids change during modeling, the host cells of interface grids in both CFD model and FVCOM are subject to change, and they need to be located at each time step during the simulation. The solution exchange at grid interfaces requires transferring solutions from host cells/elements to interface grid nodes. Tri-linear interpolation is used to facilitate the solution exchange from the CFD model to FVCOM

(e.g., Tang et al. 2006), and a linear interpolation is employed to implement solution from FVCOM to CFD at grid interfaces. The interpolations have second-order accuracy, which is consistent with the accuracy of the both models. The coupling is two-way and implemented using the Schwarz alternative procedure in the iteration between the two models (Schwarz, 1869). In order to achieve correct as well as accurate solutions at grid interfaces, it is necessary to enforce conservation of certain properties such as mass (Tang, 2006). However, this needs special treatment and will be left for future study.

4. NUMERICAL EXAMPLES

First, an effluent discharged from a diffuser into a rectangular channel is simulated (Fig. 2). The diffuser consists of a pipe and 10 discharge ports on it. The pipe is 1.32 m in diameter, it lies on the channel bottom with an angle of 110 degree to the flow direction, and its offshore end is 201 m away from the left bank. Totally 10 ports are installed on the pipe,

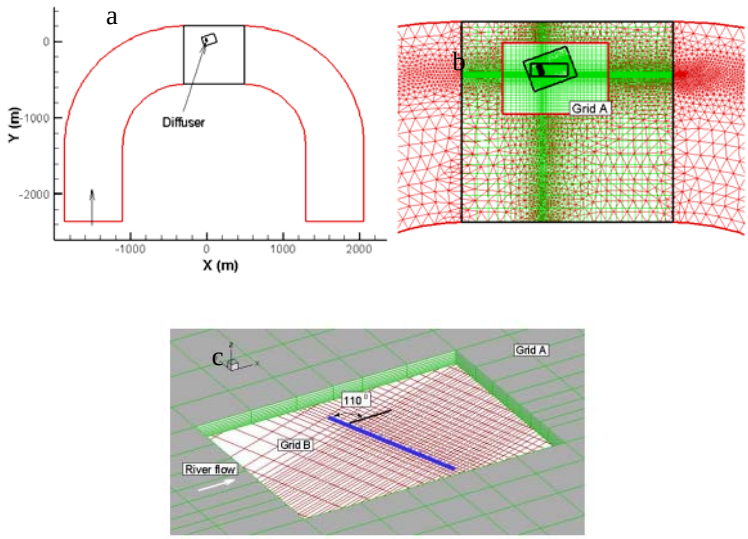

Figure 2. River bend flow with effluent discharge. a). River and diffuser. b). Mesh. Structured mesh in green– CFD, unstructured mesh in red – FVCOM. c) Mesh around the diffuser.

and they are 0.175 in diameter, 3.05m apart between each other, and with different upward angles gradually changing from 45^o to 18^o in y direction. The ambient flow is 0.3 m/s in velocity, and the depth at the exit is 16 m. The effluent is discharged at the port mouths with velocity of 3.92 m/s. Multiple layers of grids are used to fully resolve the diffuser configuration, and each port has a few grid nodes across their diameters (Fig. 2b and 2c). The grids for the CFD model have 180,000 nodes. For details on the diffuser and its CFD mesh arrangement, the readers are referred to Tang et al. (2008). The GFD uses 11 layers

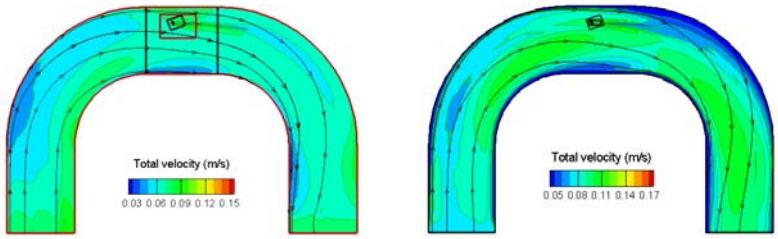

Figure 3. Solution for velocity. Left -- coupling of CFD and FVCOM (red line – FVCOM boundary, black line – CFD boundary), right -- CFD

of grids in the vertical direction with the total 115,000 nodes on each layer (Fig. 2b). The flow is also simulated by only using the CFD model with 220,000 grid nodes.

The computed flow field at a cross section 3m above the bottom of the river is presented in Fig. 3. It is seen that coupling CFD/GFD approach and CFD model alone predict similar structures of flow field, and the difference between their results is attributed to the fact that

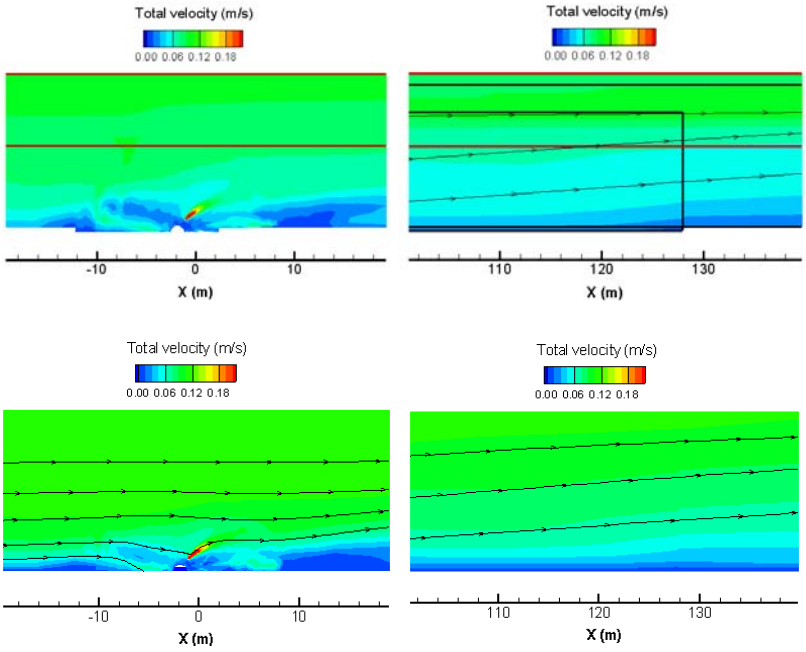

Figure 4. Top -- CFD and FVCOM coupling (red line – FVCOM boundary, black line – CFD boundary), bottom – CFD.

they use different conditions; the former has a slip velocity at the lateral walls and a free surface, whereas the latter uses a no-slip condition at the lateral walls and rigid surface. It is seen in Fig. 3 that the solution transition between CFD and GFD models is smooth, and the interface treatment preserves the flow structures there. This is further demonstrated in Fig. 4, which presents the solutions on a vertical plane crossing a discharge port. Fig. 3 and 4 also illustrate that the proposed coupling technique produces a solution similar to that provided by the CFD model.

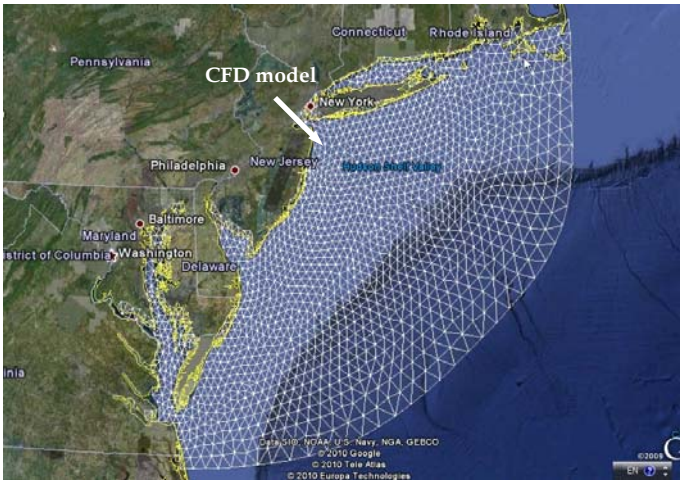

Figure 5. New York/New Jersey coast region and FVCOM mesh and CFD location

Second, the effluent discharge in the previous river flow case, with a higher temperature, is put into the setting of the New York and New Jersey coastal region under action of tides. The coastal flow and the effluent discharge are respectively 20.5 ^{o}C and 32.0 ^{o}C in temperature. The flow is simulated using the CFD and FVCOM hybrid approach, with flow domain and mesh as shown in Fig. 5. The computed solutions for the flow filed and temperature at the diffuser are presented in Fig. 6. Fig. 6a and 6b demonstrate the flow velocity distribution under flood and ebb tide conditions on a plane 3m above the diffuser, and it is clearly seen that the flow can smoothly pass the interface between CFD and FVCOM models. Fig. 6c and 6d illustrate a computed 3D view of the thermal discharge plume at flood and ebb tides.

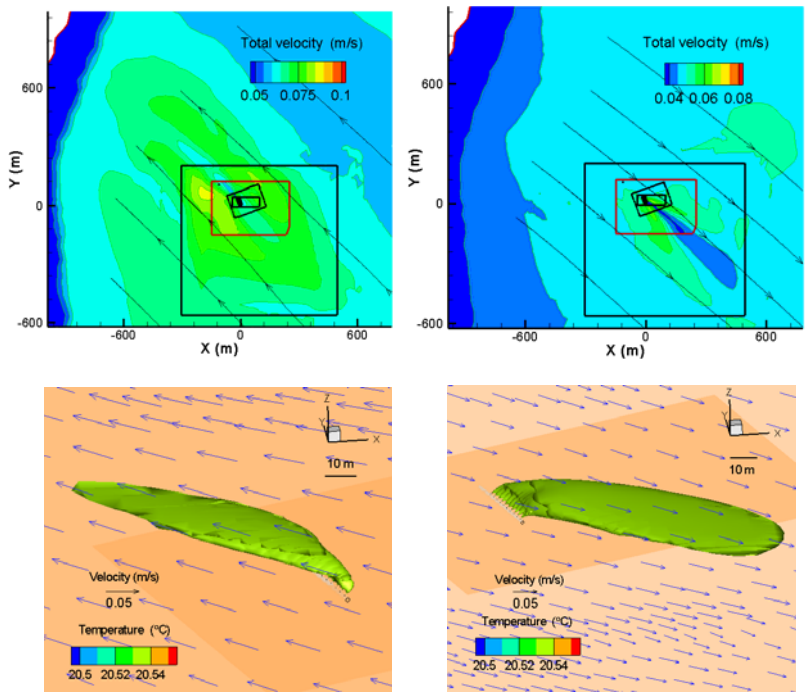

Figure 6. Solution for thermal discharge. Top – velocity field, bottom – thermal plume and water surface vectors, left – flood tide, right – ebb tide.

5. CONCLUDING REMARKS

This paper proposes to simulate multi-scale and multi-physics coastal ocean flows using CFD and GFD hybrid approach on the basis of a rigorous foundation. Particularly, DDM with Chimera overset grids is employed to couple CFD and FVCOM models. Coupling strategies are discussed and numerical examples are presented. The numerical examples demonstrate the feasibility and promising capability of the approach. It should be noted that the techniques coupling CFD and FVCOM employed in this paper are also applicable in coupling CFD with other coastal models such POM and NCOM. In order to achieve correct, accurate, and robust coupling between CFD and GFD models, important issues such as conservation at interfaces between the models will be the future study topics.

ACKNOWLEDGEMENT

This research is supported by PSC CUNY and NSFC (40806037). Valuable input from Dr. C. S. Chen at Univ. of Massachusetts Dartmouth and Dr. Timothy Keen at US Naval Research Laboratory is acknowledged.

REFERENCES

Benek, J. A. Steger, J. L. and Dougherly. F. C. (1983). A flexible grid embedding technique with application to the Euler equations. AIAA Paper 83-1944.

Blumberg, A. F. and Mellor, G. L. (1987). A description of a three-dimensional coastal ocean circulation model. In: Heaps, N. (Ed.), Three-Dimensional Coastal Ocean Models, American Geophysical Union, 1-16.

Chen, C., Liu, H., Beardsley, R. C. (2003). An unstructured, finite-volume, three-dimensional, primitive equation ocean model: application to coastal ocean and estuaries. J. Atm. & Oceanic Tech., 20:159-186.

Chen, C. S., Beardsley, R. C. and C., Geoffrey. (2006). An Unstructured Grid, Finite-Volume Coastal Ocean Model FVCOM User Manual. SMAST/UMASSD-06-0602.

Dolbow, J. Khaleel, M. A. and Mitchell, J. (2004). Multiscale Mathematics -- Initiative: A Roadmap, PNNL-14966.

Fringer, O.B., Gerritsen, M., and Street, R.L. An unstructured-grid, finite-volume, nonhydrostatic, parallel coastal ocean simulator, Ocean Modelling, 14(2006) 139–173.

Griffles, S. M.. Bo¨ning, C Bryan, F. O. Chassignet, E. P. Gerdes, R. Hasumi, H. Hirst, A. Treguier. A. M. (2000). Developments in ocean climate modelling. Ocean Model. 2, 123–192.

Halliwell, G. R. (2004). Evaluation of vertical coordinate and vertical mixing algorithms in the HYbird-Coordinate Ocean Model (HYCOM), Ocean Modeling, 7, 285-322.

Harten, A. Discrete multi-resolution analysis and generalized wavelets, Appl. Numer. Math., 12(1993), 153-192.

Heimusund, B. –O. Berntsen, J. (2004). On a class of ocean model instability that may occur when applying small time steps, implicit methods, and low viscosities, Ocean Modeling, 7, 135-144.

Kumar, P. and Foufoula-Georgiou, E. (1997). Wavelet analysis for geophysical applications, Reviews of Geophysics, 35, 385–412.

Legeckis, R., Pichel, W., and Nesterczuk, G. (1983). Equatorial long waves in geostationary satellite observations and in a multichannel sea surface temperature analysis. Bull. Am. Meteorol. Soc. 64, 133-39.

Mellor, G. L. and Yamada, T. (1974). A hierarchy of turbulence closure models for planetary boundary layers. J. Atmos. Sci., 31, 1791–1806.

Paik, J., Sotiropoulos F., and Sale, M. J. (2005). Numerical simulation of swirling flow in a complex hydro-turbine draft tube using unsteady statistical turbulence models. J. Hydr. Eng.. 131, 441-456.

Pedley, T. J. (1992). Hydrodynamic phenomena in suspensions of swimming microorganisms, Ann. Rev. Fluid Mech. 24:313-58.

Schwarz, H. A. (1869) Uber einige abbildungsaufgaben, GES. Abh., 11, 65-83.

Song, Y. T. and Hou, Y. T. (2006). Parametric vertical coordinate formulation for multiscale, Boussinesq, and non-Boussinesq ocean modeling, Ocean Modeling, 11, 298-332.

Tang, H. S. (2006). Study on a grid interface algorithm for solutions of incompressible Navier-Stokes equations, Computers & Fluids. 35, 1372-1383.

Tang, H. S., Keen, T. R., and Khanbilvardi, R. (2009). A model-coupling framework for nearshore waves, currents, sediment transport, and seabed morphology, Comm. Non-linear Sciences & Numerical Simulations, 14, 2935-2947.

Tang, H. S., Jones, C., and Sotiropoulos, F. (2003). An overset grid method for 3D unsteady incompressible flows, J. Comput. Phys., 191, 567-600.

Tang, H. S. Paik, J. Sotiropoulos, F. and Khangaokar, T. (2008). Three-dimensional CFD modeling of thermal discharge from multports. ASCE J. Hydr. Eng,, 134, 1210-1224.

Thorpe, S. A. (2004). Langmuir Circulation, Ann. Rev. Fluid Mech. 36. 55–79.

Weller, R. A., Dean, J. P., Marra, J., Price, J. F., Francis, E. A., and Boardman, D. C. (1985). Three-dimensional flow in the upper ocean. Sciences, 227, 1552-1556.